

# Solar Cell Characterization

Kai Shin

Senior Honors Thesis

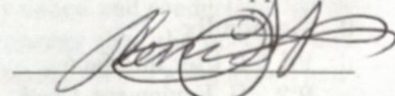
Applied Sciences

Advisor - Dr. Rene Lopez

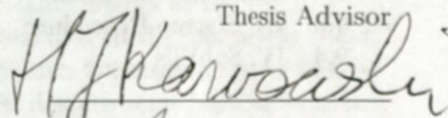
Supported by the Dunlevie Honors Undergraduate Research Award

April 10, 2015

Approved:



Thesis Advisor



Reader



Reader

# Contents

<b>1</b>	<b>Abstract</b>	<b>3</b>
<b>2</b>	<b>Devices to be Characterized</b>	<b>3</b>
2.1	DSSC's and Liquid Electrolyte Cells . . . . .	4
2.2	Dry Cells . . . . .	5
<b>3</b>	<b>Characterization Techniques</b>	<b>6</b>
3.1	I-V Curve Analysis . . . . .	6
3.2	EIS . . . . .	7
3.3	IPCE Measurement . . . . .	10
<b>4</b>	<b>Hardware</b>	<b>10</b>
4.1	Cell Holder Attachments . . . . .	11
4.2	Motion . . . . .	12
4.3	Incident Light . . . . .	12
4.4	I-V Curve Analysis and EIS . . . . .	13
4.5	IPCE Measurement . . . . .	14
4.6	Path Switching . . . . .	16
<b>5</b>	<b>LabVIEW</b>	<b>17</b>
5.1	Data Recording . . . . .	18
5.2	Sample Path Determination . . . . .	19
5.3	Motor Control . . . . .	20
5.4	I-V Curve Analysis . . . . .	21
5.5	EIS . . . . .	22
5.6	IPCE Measurement . . . . .	22
<b>6</b>	<b>Experimental Procedure</b>	<b>23</b>
<b>7</b>	<b>Conclusion and Next Steps</b>	<b>24</b>
<b>8</b>	<b>References</b>	<b>26</b>
<b>9</b>	<b>Appendix</b>	<b>28</b>
9.1	I. User Interface . . . . .	28
9.2	II. Equipment Used . . . . .	31
9.3	III. Startup Procedure . . . . .	32
9.4	IV. SubVI's . . . . .	34

# 1 Abstract

Recent decades have witnessed a growing shift away from fossil fuels as their harmful effects and dwindling supply have become more acute. As attention has turned towards alternative energy sources, solar energy has shown promise as a potentially complete solution. Sunlight can be captured and converted directly into usable electrical power via photovoltaic devices as well as create liquid, combustible Hydrogen fuel from water through a process called hydrolysis.<sup>1</sup> Understandably, a massive amount of research is being done on developing efficient devices for economic application as soon as possible. The University of Chapel Hill serves as an Energy Frontier Research Center where researchers are developing a number of different solar devices. These range from Dye Sensitized Photoelectrosynthesis Cells (DSPEC's), which require a liquid electrolyte that may one day be used to capture sunlight to create Hydrogen fuel,<sup>2</sup> to graphene/GeSi quantum dot dry cells<sup>3</sup>. Accommodating the large number being produced requires a method for efficient characterization of the devices. Cells are typically characterized through a number of different tests, which are currently done one at a time at several different locations resulting in an inefficient, time consuming process.

This thesis focuses on addressing this pain point through the development of a multi-path characterization device that can perform several different tests automatically without continuous manual input by the researcher. Referred to as the Solar Automated Multi-Meter (SAMM), the resulting apparatus supports three formats of photoactive cells: cells that require liquid electrolyte, and two formats of dry cells, one in which the anodic and cathodic contacts lie on the same side of the cell and one in which the contacts are on opposing sides. Programmed using National Instrument's LabVIEW, the SAMM can perform three distinct types of measurement at multiple locations on each cell: I-V curve generation, EIS, and IPCE measurement.

## 2 Devices to be Characterized

At the most basic level, all semiconductor-based solar cells function the same way. A semiconductor is a material with a bandgap between the valence and conduction bands of the electrons where the conduction band is at a higher energy than the valence band and the bandgap is the energy difference between the two levels. When a semiconductor is exposed to light, the incoming photons that have the same energy as the bandgap are absorbed by electrons occupying the valence band, and excited to the conduction band.<sup>4</sup> These electrons can then be used to power electronic circuits (photovoltaics) or fuel hydrolysis (photoelectrochemical synthesis cells). However, despite some basic similarities, solar devices fabricated by researchers come in a variety of different formats. One issue with the current characterization infrastructure is that separate methods must be used for each solar cell format. Thus, effort was made to allow for the easy interchange of different solar devices. Three basic device structures were considered: cells requiring a liquid electrolyte component, dry cells with the anodic and cathodic contacts on the same side of the cell, and dry cells in which the contacts are on opposite sides of the cell.

## 2.1 DSSC's and Liquid Electrolyte Cells

The bandgap of many semiconductors is actually greater than the energy in photons in most of the visible range which means that a large portion of sunlight goes unused as the cells will primarily absorb UV light. To address this, researchers have coated cells in a chromophore dye that is chemically designed to absorb more of the wavelengths present in sunlight. DSSC's are of high interest because they have low production costs, have great flexibility in shape, color, and transparency, and show promise in real outdoor conditions.<sup>5</sup>

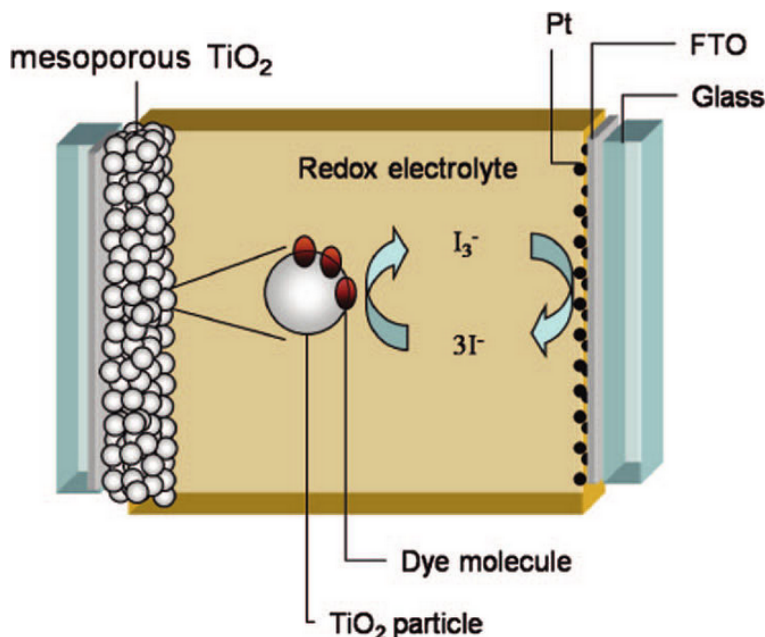


Figure 1: The structure of a typical, self-contained DSSC device. The cell shown here is oriented so that the dye sensitized anode is on the left. Incident light would come from the left. The SAMM's liquid electrolyte cell attachment would include the platinum cathode and contain the electrolyte so that researchers can load just the dye sensitized film of metal oxide on the conductive substrate (figure credit Gao et al)<sup>6</sup>

As shown in figure 1, a typical DSSC anode has three important parts: the metal oxide that serves as the primary semiconductor, the dye coating which amplifies absorbance at specific wavelength ranges, and the electrolyte which replaces the electrons of the dye as they are excited to prevent molecular breakdown. One particular type of dye sensitized cell that the UNC EFRC has been interested in is a dye sensitized photoelectrochemical synthesis cell, or DSPEC. DSPEC devices differ from typical DSSC's in that the excited electrons are not used directly as electricity. Instead, the electrons are used to hydrolyze water into its component Hydrogen and Oxygen atoms. For the purposes of DSPEC devices, the metal oxide and dye are specifically chosen so that the bandgap of cell is approximately equal to the activation energy of hydrolysis. This allows the excited electron to be injected directly into the hydrolyzing reaction without the need for additional power supplies. The result is a solar powered device that automatically creates H<sub>2</sub> and O<sub>2</sub> rather than producing electricity. The metal oxide, most commonly Titanium Oxide or TiO<sub>2</sub>, is deposited onto a conductive substrate using methods like Pulsed Laser Deposition<sup>7</sup>.



The metal oxide is then coated with the dye to complete the anode. In a self contained DSPEC, the anode is then sealed using a plate of FTO covered, conductive glass and electrolyte is injected into the space between the two plates which become tedious when working with large numbers of samples. The SAMM accounts for this inconvenience through cell holder that can contain the liquid electrolyte and platinum cathode. Thus a dye coated cell could be loaded without the need to make it a self contained device.

## 2.2 Dry Cells

Two formats of dry cell have been anticipated: one in which the anodic and cathodic contacts are on the same side of each cell, and one in which the contacts are on opposite sides of each cell. An example of a dry cell with one sided contacts are the  $\text{TiO}_2$  photoanodes produced by Ghosh et al<sup>7</sup>. These photoanodes, created using the PLD technique on transparent FTO, can be used as the metal oxide base of a dye sensitized cell or tested independently to isolate the behavior of the  $\text{TiO}_2$  nanofilms from the complicating effects of the dye loading and electron injection. The PLD method uses a pulsed laser to ablate a plume of target metal oxide which is then aimed at the FTO substrate to create 'nanoforest' structures of metal oxide. The pressure and temperature of the deposition environment, the distance between the substrate and target, as well number of laser shots used to create the film, all have significant effects on the behavior of the cell. Additionally, the target material to be ablated can be alternated to dope the metal oxide with various concentrations of dopants. These dopant levels can even be deposited in a gradient across a single cell by precisely aiming the ablated plume during deposition. With the right mask placed in the path of the ablated plume, this technique can be used to create multiple distinct anodes on a single cell each with different levels of dopant and thus distinct photo-active characteristics. The anode connections are made at each of deposited areas while the common cathode connection can be made at any point of the cell not coated in metal oxide. This allows all of the electrode connections to be on the same side, usually opposite the incident light to avoid any blockage of incoming light.

However, this is only possible because the substrate, Flourine-doped Tin Oxide (FTO) in the case of figure 1, is transparent and thus allows light to be absorbed from either direction. Figure 2 shows the difference between cells created out of transparent and opaque materials.

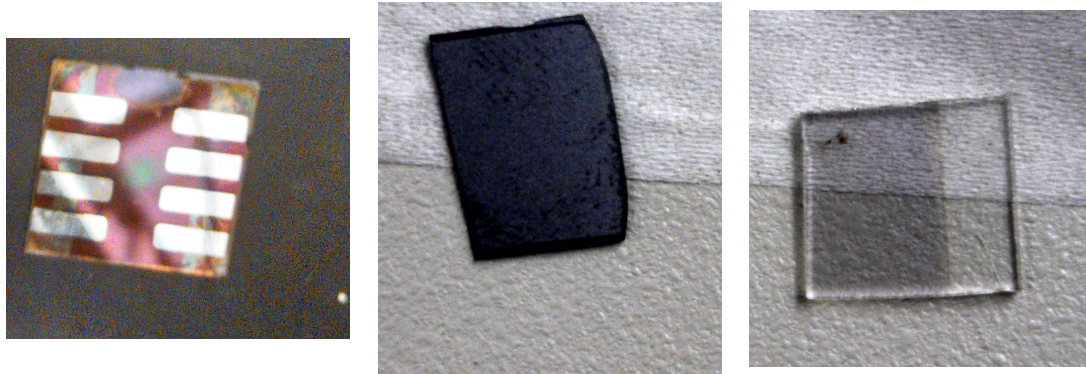


Figure 2: **left** A cell showing multiple discrete anodes that can be fabricated using a mask during deposition **center** Cell made from opaque Si substrate **right** Film deposited on transparent FTO glass (photo credit to Kai Shin)

For cells created on a Silicon substrate or other opaque materials, the anodic connection must be on the illuminated side. An example of this kind of cell are the graphene/GeSi quantum dot hybrid cells produced by Chen et al<sup>3</sup>. While it is possible to have the cathodic connection on the same side as the anodic connection (it just would have to go on an area that has no film deposited so the connection can be made directly to the substrate) for the purposes of constructing the SAMM it was decided that having too many electrodes on the same side as the incident light created unnecessary potential for blocking the light before it reached the cell itself.

### 3 Characterization Techniques

The performance of a solar cell is based upon a multitude of different factors and so requires many different tests to fully characterize. The SAMM supports three distinct methods of characterization: I-V Curve Analysis, EIS, and IPCE measurement.

#### 3.1 I-V Curve Analysis

An I-V curve is generated by applying a variable voltage and measuring the resulting current. In the context of solar devices, this is performed in both dark and illuminated conditions. The resulting curves are compared to measure how much DC voltage is produced by the cell upon illumination. Figure N shows several IV curves generated using different light sources aimed at a standard Thorlabs SM1PD1B photoactive diode. Typically, the applied voltage is scanned through a range of voltages typically from -1 V to +1 V. At low negative voltages, a negative current is observed. For an illuminated solar cell, as the voltage increases, the measured current eventually becomes positive at the point known as the open circuit voltage ( $V_{OC}$ ). This is the voltage at which the negative applied voltage exactly equals the opposing DC voltage produced by the illuminated cell causing all the excited charges to recombine within the solar cell. This creates a zero-current or open circuit scenario. As the voltage continues to increase towards zero volts, the current increases until it reaches an upper limit at which point the current is entirely due intensity of incident light and the efficiency of the cell at those wavelengths and is independent of the applied voltage. This current limit is called the short circuit

current ( $I_{SC}$ ) and is equivalent to the current the illuminated cell can produce when there is no charge carrier recombination within the cell. This is equivalent to there being zero resistance, or a short circuit, between the anode and cathode.<sup>8</sup> Multiplying these two values together gives  $P_{ideal}$ , the maximum power the cell can produce under ideal conditions. In reality, an IV curve is not rectangular, and so the knee of the curve never reaches out to the theoretical  $P_{ideal}$ . The voltage and current at the knee of the curve can be multiplied together to give  $P_{max}$ , the actual maximum power produced by the cell. The ratio of  $\frac{P_{max}}{P_{ideal}}$  gives the fill factor (FF) where an ideal cell would display  $FF = 1$ .

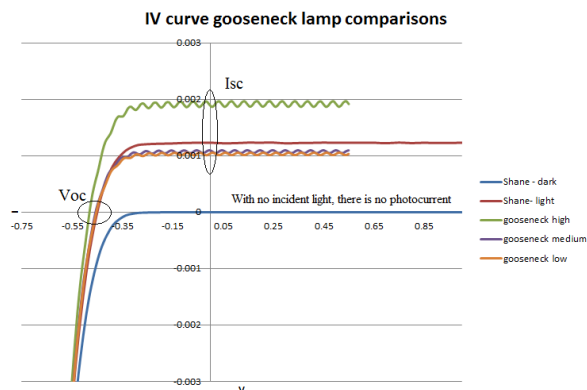


Figure 3: V Sample IV curves taken using a Thorlabs SM1PD1B diode and several different light sources. The blue curve shows an IV curve taken in dark conditions with no photoactive current being produced.

Figure NA shows some sample IV curves taken while illuminating the standard Thorlabs SMPD1B diode with different intensities of white light. The differences between the curves are due to varying intensities of incident light while the small oscillations in the current are due to a slight oscillation in the light source intensity. Additionally, the wavelengths of the incident light will affect the resulting IV curve. If the incident light is not at a wavelength that is readily absorbed by the solar cell, then there will be little photoactive current, no matter how intense the light is.

### 3.2 EIS

Electrochemical Impedance Spectroscopy (EIS) is a method of characterizing the internal impedance,  $Z$ , of the cell. Similar to an IV curve, EIS applies a voltage and measures the resulting current. However, instead of a DC voltage, EIS utilizes the application of an AC signal.<sup>9</sup> The impedance of a solar cell comprises both the ohmic resistance of the conductive pathway as well as the capacitance and inductance of material interfaces and charge depletion layers within the cell. The cell is exposed to white light, creating a DC bias, on top of which a small sinusoidal signal is applied over a large range of frequencies (usually 1 Hz to 1 MHz). This excitation signal has the form

$$E_t = E_o \sin(\omega t) \quad (1)$$

where  $E_t$  is the potential at time  $t$ , and  $\omega$  is the frequency in radians. The frequency in hertz,  $f$ , is given by

$$\omega = 2\pi f \quad (2)$$

The current resulting from this excitation is phase shifted and given by the equation

$$I_t = I_o \sin(\omega t + \phi) \quad (3)$$

where  $\phi$  is the magnitude of the phase shift.

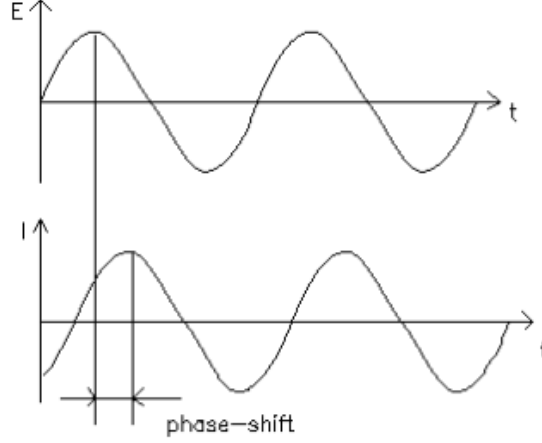


Figure 4: The phase shift between an applied AC excitation voltage and the resulting, phase-shifted current<sup>9</sup>

Despite the fact that capacitive and inductive impedance is non-ohmic, an expression analogous to Ohm's law can be used to generate

$$Z = \frac{E_t}{I_t} = \frac{E_o \sin(\omega t)}{I_o \sin(\omega t + \phi)} = Z_o \frac{\sin(\omega t)}{\sin(\omega t + \phi)} \quad (4)$$

Plotting the excitation signal  $E_t$  on the x-axis and the responding sinusoidal current  $I_t$  on the y axis results in an oval graph called a Lissajous curve.<sup>9</sup>

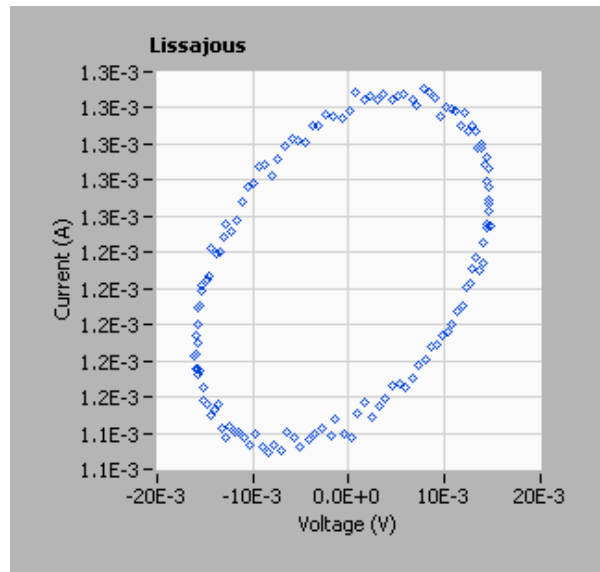


Figure 5: A Lissajous curve created using the SAMM and the Thorlabs SM1PD1B diode

Using Euler's relationship

$$e^{i\phi} = \cos(\phi) + i\sin(\phi) \quad (5)$$

it is possible to rewrite the equations for  $E_t$  and  $I_t$  as

$$E_t = E_o e^{i\omega t} \quad (6)$$

$$I_t = I_o E^{i\omega t - \phi} \quad (7)$$

which means that the impedance can be rewritten as

$$Z(\omega) = \frac{E_t}{I_t} = Z_o e^{i\phi} = Z_o \cos(\phi) + i\sin(\phi) \quad (8)$$

Plotting the real part of equation on the x-axis and imaginary part on the y-axis gives a Nyquist plot where each point on the curve corresponds to the impedance of the cell at a single frequency. The impedance at any frequency can be thought of as the magnitude of the vector from the origin to the point on the Nyquist plot that corresponds to that frequency. Nyquist plots can then be approximated as simple RC or RLC circuits for quantitative description. Depending on the cell being tested, the Nyquist plot can take the shape of some or all of a semicircle. oftentimes the curvature of the plot is not visible and so the plot can appear linear.<sup>9</sup>

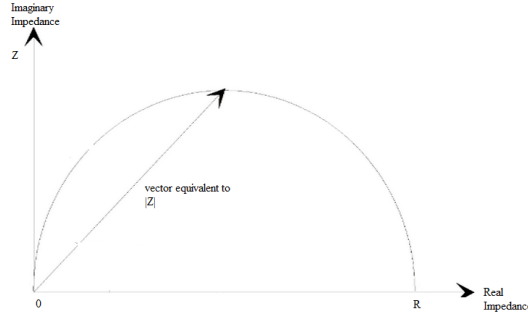


Figure 6: A diagram of a typical Nyquist Plot<sup>8</sup>

However, it is not obvious on a Nyquist plot which frequency each data point corresponds to so this data is often represented in another format called a Bode plot. A Bode plot shows both the absolute value of the impedance and the phase shift on the y-axis against the logarithm of the frequency on the x-axis. Unlike the Nyquist plot, the Bode plot clearly shows the effect of frequency on impedance.<sup>9</sup>

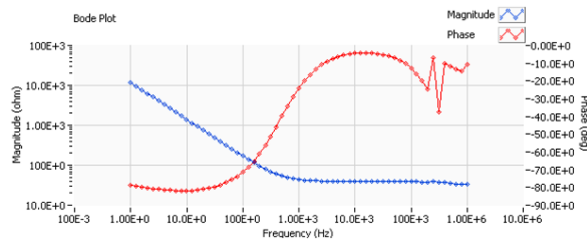


Figure 7: A Bode plot generated using the SAMM and the Thorlabs SM1PD1B diode

### 3.3 IPCE Measurement

The Incident Photon-to-Current Conversion Efficiency (IPCE) of a solar cell is a measure of the efficiency of a solar cell at specific wavelengths of incident light. This is accomplished by illuminating the cell with monochromatic light under either dark or sun biased conditions and measuring the response.<sup>5</sup> In practice, the SAMM performs this measurement by exposing the cell to monochromatic light that scans from 350 nm to 1150 nm. The current produced is then converted to a voltage and measured as a function of the wavelength of incident light. Figure N shows an example IPCE curve using the Thorlab SM1PD1B diode in both dark conditions and under a one sun bias.

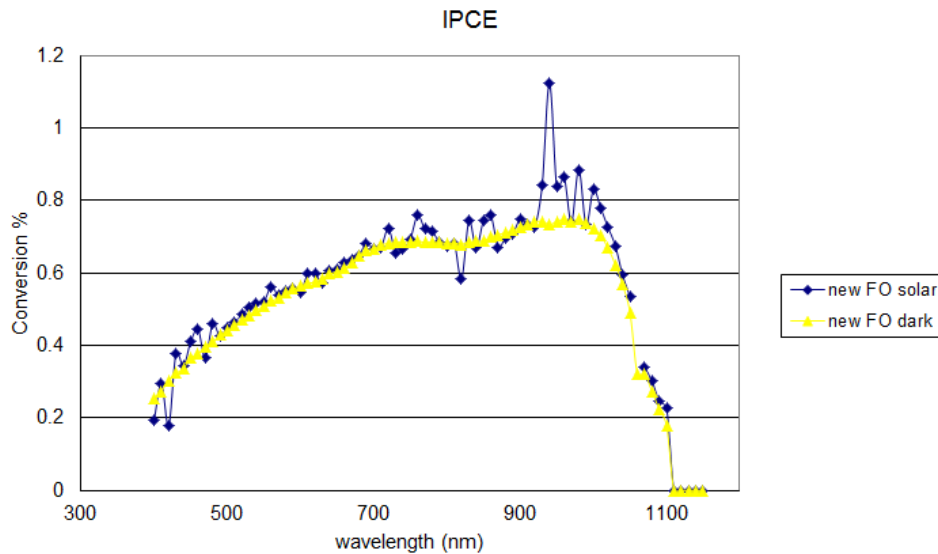


Figure 8: IPCE measurements as a function of the wavelength of incident light under both dark (yellow) and sun biased (blue) conditions.

## 4 Hardware

The SAMM apparatus incorporates several different pieces of hardware. A full list can be found in Appendix II. Below is a description of the most significant pieces to each area of operation of the SAMM.



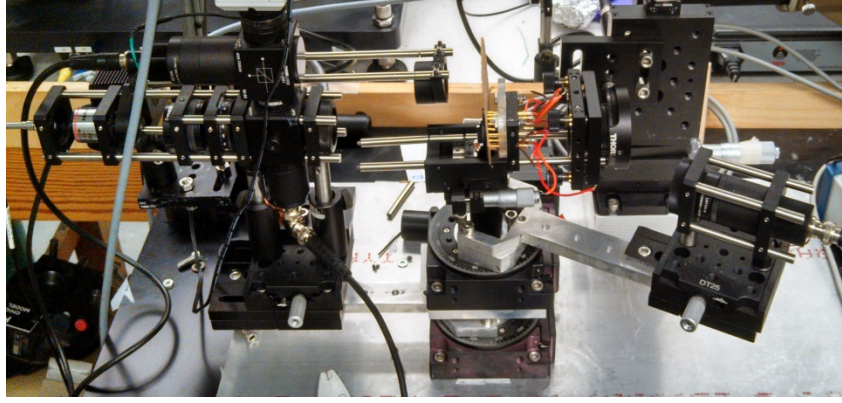


Figure 9: The SAMM apparatus. On the left side is the light source arm which can rotate in and out of the plane of the page. Sample cells are loaded into their respective holding attachments at the center of the apparatus at the focal point of the rotating arm. These holders are connected to the translational motors for cell test location determination

Not shown in figure 9 is a National Instruments DAQ 6221 device controlled through LabVIEW that is used to communicate with each piece of equipment. This device also handles the data acquisition for IPCE measurements through an analog voltage input pin. The 6221 functions by producing programmable digital and analog outputs that are used to directly control the MWFFH1 sunlight simulating diode, the custom stepper motor that controls the rotational arm, and all of the ELK path switches.

## 4.1 Cell Holder Attachments

Three interchangeable sample attachments are supported by the SAMM. A reference Thorlabs SM1PD1B diode may be screwed into the base at the focal point of the light sources. This diode is used to calibrate the IPCE data and hardware as well as troubleshoot any problems that may arise. The other two attachments are for dry or liquid electrolyte cells and are slotted into place on the opposing translational stage. This stage is connected to the two Thorlabs translational motors that move the cell so that only one user specified active site is illuminated at a time. The dry cell holder supports anodic connections on both the front (for opaque cells) and back (for transparent cells). The liquid electrolyte cell holder consists of two parts. The first contains the electrolyte reservoir as well as slots for the cathode, typically a platinum electrode, to be inserted. The reservoir opens to a square aperture rimmed with adhesive rubber that forms the seal between the electrolyte and the cell. The second part of the attachment is the casing that is screwed onto the front clamping the cell to the first piece. This part has a square aperture cut as well to allow the light to strike the surface of the cell.<sup>10</sup> The Figure 10 shows three attachments together.

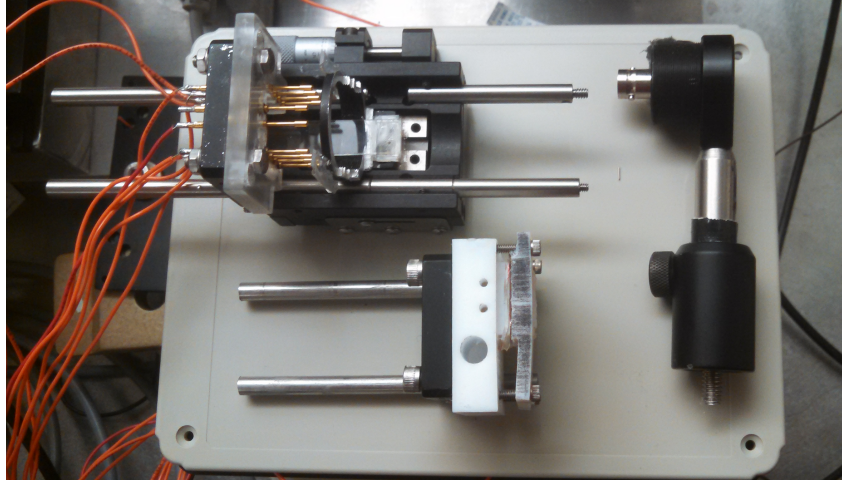


Figure 10: The three interchangeable attachments for each of the supported device formats. **Top Left** Cell holder for both formats of dry solar cell. The orange wires are connected to the individual electrodes for each distinct active photoanode site. **Bottom Left** Cell holder for the liquid electrolyte cells **Right** the SM1PD1B that is used for calibration of the IPCE measurement

## 4.2 Motion

The SAMM incorporates two different motion regimes into its operation: the translational motion of the cell holder and the rotational motion of the light source arm. The translational motion is performed by two Thorlab T-cube Stepper motor controllers each manipulated through . The rotational motion of the light source arm is powered by a custom built stepper motor and controlled through LabVIEW as well.

## 4.3 Incident Light

The types of measurement being incorporated into the SAMM required two distinct types of light source: a broad spectrum white light to simulate the sun bias and a tunable monochromatic light for wavelength specificity. A high power Thorlabs LED1B diode driver with an MWWFHI Warm White diode was used to simulate sun bias for its simplicity to control through LabVIEW and for its broad spectrum of wavelengths that approximated actual sunlight. Figure 11 shows the spectrum of light emitted from the Warm White diode compared with a standard solar spectrum.

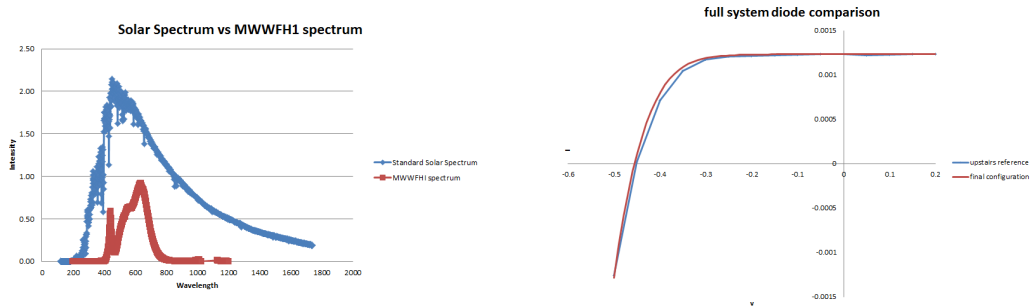


Figure 11: **Left** standard spectrum of real sunlight (blue) compared to the spectrum produced by the MWWFH1 diode used to simulate sunbias for the SAMM<sup>11 12</sup> **Right** IV curve showing that the white diode used to simulate 1 sun bias produces the same curve as standard solar simulator

As shown in figure 11 though, the light produced by the MWWFH1 diode is not as intense as real sunlight at without further focusing. To compensate, the light emitted by the MWWFH1 diode was passed through a series of lenses to focus the incident light at the cell to the intensity of real sunlight. This arrangement was determined by comparing the IV curves generated by the reference SM1PD1B diode at various levels of focus to an IV curve generated by the same reference diode using the CHANL solar simulator. Figure 11 shows the close approximation that was achieved using this method.

The monochromatic light is produced by a Woollam VASE monochromator which is part of a separate ellipsometry apparatus. In order to control the monochromator through LabVIEW, it is necessary to remote connect to the computer dedicated to that station. This wavelength specific light has a sinusoidal behavior due to a mechanical chopper within the monochromator. This chopper pulses the light at approximately 270 Hz. This frequency specificity is what allows the signal resulting from monochromatic excitation of the test cell to be filtered out from the DC bias of the MWWFH1 diode during a sun biased IPCE measurement. The light emitted by the monochromator is passed through a beam splitter before being exposed to the cell to form a standard two-path system. One of the beams is passed onto the sample being tested while the other is fed to a reference Thorlabs SM1PD1B diode. Because the monochromator cannot produce equally intense light at all wavelengths, this diode provides information about the baseline intensity of each wavelengths. This data is used to correct for the magnitude differences in the resulting photocurrent of the test sample. Without this correction, the IPCE measurements would be unreliable because the test sample might produce a strong photocurrent at a wavelength it really doesn't absorb very well simply because the monochromator happens to produce very intense light at that wavelength.

## 4.4 I-V Curve Analysis and EIS

Both the IV curve and EIS tests call for the use of a Gamry REF-600 potentiostat, a device capable applying precise voltages and making very precise current and voltage measurements using a variety of different electrode connection schemes. For the purposes of the two tests included in the SAMM, a simple two connection scheme is adequate in which connections are made only at the anode and cathode of the cell. This device is communicated to via LabVIEW. Both of these test also call upon the use of the MWWFH1 Warm White diode for illumination.

## 4.5 IPCE Measurement

IPCE measurement is the most complex of the characterization techniques included in the SAMM apparatus simply because it requires the most individual pieces of equipment. The need for both sun biased and dark condition measurements means that the IPCE sequence uses both the monochromator, the MFWFH1 diode, and the rotational arm to position the light sources mid-sequence. Because IPCE measurements require a two path setup to compensate for intensity variations between wavelengths, two separate data acquisition paths have been constructed, one for the sample being tested, and one for the reference SM1PD1B diode that provides the baseline intensity data. The reference SM1PD1B diode is therefore only exposed to monochromatic light which is relatively weak compared to the white light used for sun bias. This means the resulting oscillating current is generally small and so the signal is first passed through a Portable Technologies Transimpedance Amplifier which converts the current to a voltage and then amplifies it so it can be measured directly by the DAQ 6221.

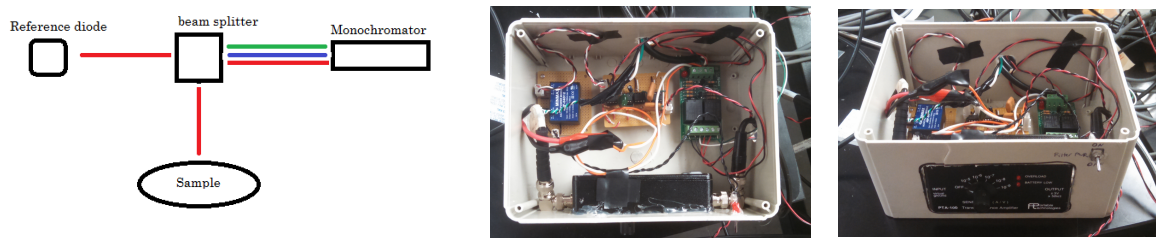


Figure 12: **Left** A diagram of the two path nature of the IPCE measurement **Center** Project box containing the circuitry for IPCE measurements: Portable Technologies transimpedance amplifier, MIN-MAX dual output power supply, custom amplifying filter circuit, and ELK 924 to switch between IV and IPCE pathways **Right** Angled image of project box to show user operated switches. Transimpedance amplifier must be set to desired sensitivity and power switch must be flipped on before IPCE measurements can be made

The signal produced by the sample is treated differently however. It was found that the SM1PD1B diode used to calibrate the IPCE hardware produced a strong enough current under sun bias to overload a transimpedance amplifier even at its least sensitive setting. A separate amplifying filter circuit was constructed to filter out the oscillating signal caused by the monochromatic light out of the DC bias caused by the sun bias is shown in figure 13. This circuit was powered by a MINMAX  $\pm 12$  V power supply. The target frequency isolated by the circuit is 258 Hz, close to the frequency at which the monochromatic light is being chopped. This chopping results in an oscillating photoactive signal from any sample. The frequency to look for was determined by exposing a Thorlabs SM1PD1B diode to the monochromatic light, passing the resulting signal through a transimpedance amplifier and then feeding into the DAQ 6221 as an analog input. Using LabVIEW's Fourier transform VI, this signal was split into its component frequencies. The monochromator's frequency was then simply the one that changed in magnitude as the wavelength of the monochromator was changed which was observed to be 272 Hz.

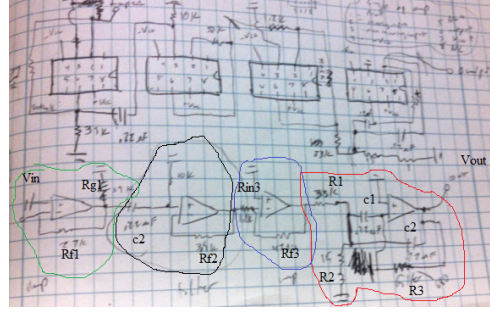
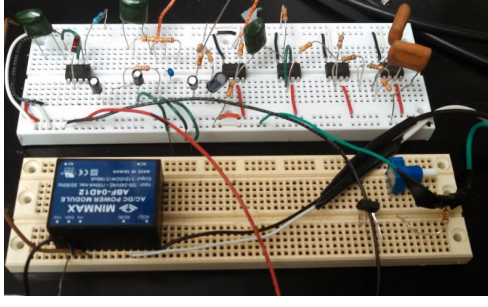


Figure 13: **Left** A presoldered version of the modified filter circuit used to pick out the wavelength dependence of the cell's response to monochromatic light. The blue box in the lower left is the MINMAX dual output power supply **Right** Circuit diagram outlining the structure of the circuit. Stage 1 is outlined in green, stage 2 in black, stage 3 in blue, and stage 4 in red

The circuit consists primarily of four LF411 operational amplifiers in series. Each amplifier forms a distinct step in signal acquisition process. The signal coming from the sample cell in a sun biased measurement consists of a large DC offset caused by the sun bias with a small oscillating signal caused by the chopped, monochromatic light superimposed on top. The first stage is simple transimpedance amplifier in which a large feedback resistance  $R_f$  converts the photoactive current of the sample cell into a voltage output. The gain of this stage is the ratio of  $R_f$  and  $R_g$  <sup>13</sup>

$$-A = \frac{R_f}{R_g} \quad (9)$$

which is determined by the value of the resistor connecting the output to ground.<sup>13</sup> Because the signal is passed into the inverting input, the gain is negative. Values of  $R_f = 10 \text{ k}\Omega$  and  $R_g = 5 \text{ k}\Omega$  were selected to give a gain of 2. It was important to keep the gain relatively low to avoid saturating the amplifier's output. In this case, because the power supply voltage is 12V, the gain was selected so that the output voltage never exceeded 12V. With a gain of 2, the output voltage of stage 2 was measured to be 4 V using the SM1PD1B diode under full sun bias. During actual experimentation, this is the maximum illumination that a cell will receive. Under full sun bias and without further filtering, the oscillating signal from the monochromatic light is too weak to be observed at this stage.

The second stage is a non-inverting unity gain high pass filter which removes the DC offset portion of the signal and passing only the high frequency signal due to the monochromatic incident light. The corner frequency of this filter is given by

$$f_c = \frac{1}{2\pi RC} \quad (10)$$

Values of  $10 \text{ k}\Omega$  and  $0.22 \text{ }\mu\text{F}$  were selected to give  $f_c = 72 \text{ Hz}$ . This is sufficiently high to exclude the DC offset caused by the sun bias but low enough to pass the 270 Hz signal due to the monochromatic light without attenuation. The output of this stage is a weak, noisy 270 Hz signal on the order 0.01 mV that is due solely to the monochromatic light and any high frequency noise present in the signal. The exact amplitude changes based on intensity variations between wavelengths. However, the signal is too noisy to allow for accurate measurement.

Stage 3 is a simple negative feedback amplifier which inverts the signal again back to its

original orientation. The gain of this amplifier is high since the part of the signal that is due to the oscillating monochromatic light is weak. The gain of this stage is given by <sup>13</sup>

$$-A = \frac{R_f}{R_{in}} \quad (11)$$

$R_f$  was chosen to be 100 k $\Omega$  while  $R_{in}$  was chosen to be 1k $\Omega$  for a gain of 100x. At the output, an approximately 10 mV oscillating signal is observed although it is still too noisy to be reliable.

Stage 4, a multiple feedback bandpass filter, performs the final signal scrubbing to isolate the desired 270 Hz signal by removing the remaining high frequency noise. The center frequency of this filter is given by <sup>14</sup>

$$f_c = \frac{1}{2\pi} \sqrt{\frac{1}{R_3 c_1 c_2} \left( \frac{1}{R_1} + \frac{1}{R_2} \right)} \quad (12)$$

Actual values for  $R_1$ ,  $R_2$ ,  $R_3$ , and  $c_1$ ,  $c_2$  are 15 k $\Omega$ , 270  $\Omega$ , 30 k $\Omega$ , and 0.22 $\mu F$  respectively where  $c_1 = c_2$ . This gives a corner frequency  $f_c = 258$  Hz. The output of this stage is fed directly into the DAQ 6221 as the collected data. Each voltage corresponds to the sample cell's photoactive current resulting from monochromatic light at a particular wavelength.

## 4.6 Path Switching

Because there are so many different test methods and possible connections from each of the cell holder attachments, a significant amount of hardware is dedicated to signal pathway determination. The two devices used for this purpose are ELK 924 low current trigger switches and PCI 6520 relays. The PCI relays consist of three sets of NC, COM, and NO pins, five sets of NO, COM pins, and 16 trigger pins. <sup>15</sup> One of these PCI relays is used to switch between the possible pathways for a cell with multiple discrete active areas. Currently the SAMM has the capability to measure eight different active sites on one dry cell.

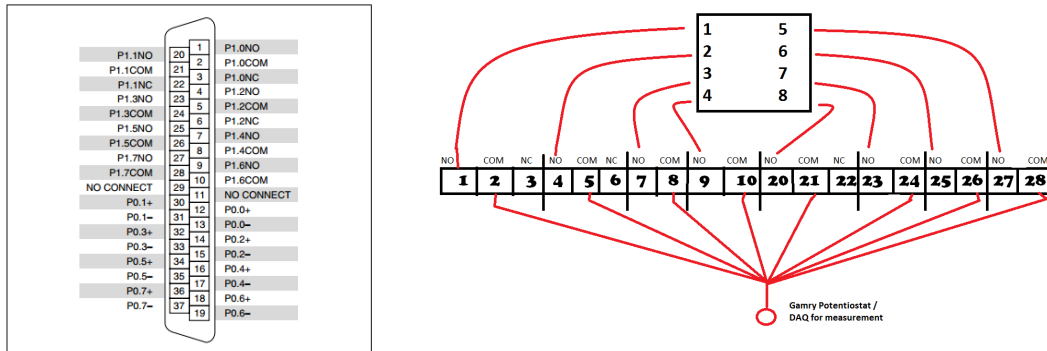


Figure 14: **Left** Connection diagram for the PCI 6520 relay **Right** sketch showing how connections to each active site are connected through the PCI 6520 terminal block so that only one is connected at a time <sup>15</sup>

Each ELK consists of two separate switches with NC, COM and NO pins. The default setting is for NC and COM to be connected while NO is disconnected. <sup>16</sup> When



a 5V trigger signal is received at the trigger pin, the connections switch so that NO and COM are connected and NC is disconnected. The SAMM uses the DAQ 6221's LabVIEW controlled digital I/O lines to produce these trigger signals. One ELK 924 is used to switch between the output connections to the Gamry REF-600 potentiostat for IV/EIS measurement and the DAQ 6221 for IPCE measurement. Shown in figure 14, this is done by connecting both IV/EIS connections to the NC pins of each switch and the IPCE connections to the NO pins. The COM pins are connected to the sample's anode and cathode connections.

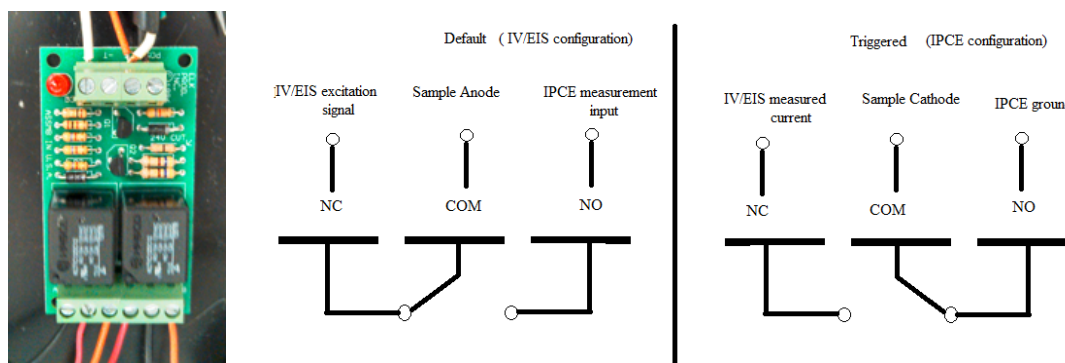


Figure 15: **Left** An ELK 924 switch. On the left are the power and trigger inputs, on the right are the two sets of NC, COM and NO pins **Right** path diagram showing the how the ELK 924 is used to switch between IV/EIS and IPCE measurement pathways

Three other ELK 924 switches, along with one PCI 6520 relay, are used to switch between the different anode and cathode connections of the cell holder attachments. These switches are made depending on what cell holder the user specifies. Each possible anode and cathode connection is connected to a NO pin on one of the switches. When a particular cell type is specified, a trigger signal is sent by the DAQ 6221 to the appropriate switch to connect COM and NO while the others remain disconnected.

## 5 LabVIEW

The functionality of the SAMM apparatus is entirely programmed through National Instrument's LabVIEW. The overarching program or Virtual Instrument, that runs the SAMM will be referred to as *Framework.vi*. The main experimental operations consist of a sequence of four steps:

- The first step is for the organization of the numerous controls, indicators, and variables that will be used throughout the program
- The second handles experimental parameter selection and IV curve analysis if that is one of the measurements that is being performed
- The third stage oversees EIS
- The fourth stage handles both IPCE calibration and actual IPCE measurement as well as general cleanup once cell testing has been completed.

Framework.vi calls upon several other subVI's for repetitive or complex operations. A full list of these subVI's can be found in Appendix IV. The front panel of *Framework.vi* forms the user interface and is tab structure with five different pages that can be viewed. There is one set up page where users can input the type of cell they want to measure and where exactly on the cell to test before initiating data collection. This is accomplished in the form of boolean controls which correspond to particular locations on a cell according to the diagram on the front panel. Toggling those controls TRUE or FALSE determines which locations are tested and thus which anode/cathode connection should be connected and used to collect data. The other four are allow the user to control the parameters of each of the three test procedures with the additional page being dedicated to IPCE calibration. Appendix I shows each of the pages in the tab structure on the front panel. When *Framework.vi* is executed, it allows the user to input all of the desired parameters for their experimental sequence like what tests to perform, what cell type they are using, and what locations to test. When the START button on the main page on the front panel is toggled, the program performs one test at each of the locations specified, then moves on to the next test and repeats for each location. The locations are isolated by moving the sample itself so that the incident light is directed at the appropriate active site.

## 5.1 Data Recording

The subVI, *new SAVE.vi* handles the organization of the data to be saved during each test. It does this by attaching identifying tags to the file name determined by the user that specify the location on the cell being tested. Consideration was given to the fact that users may want to test cells that aren't necessarily adjacent or in a particular pattern. The subVI cannot simply just assume that the first location tested is the same each time a cell gets tested. *new SAVE.vi* accomplishes this by taking the boolean information about each cell and converting it into four arrays of TRUE/FALSE values. These arrays represent the target sites for the IV tests, EIS measurements, and dark and sun biased IPCE measurements to perform during one experimental sequence. After each location is visited during one of the tests *new SAVE* is called on again to update the cell target locations to be visited by removing the site that was just tested from the array for that particular test. It works by creating arrays of the cell location to be tested for each of the different characterization methods. As each data set is recorded, the program scans through each array and adds the appropriate tag for the first location it encounters ('cell 1' for location 1 etc). Once it saves a data set using the tag, it sets that value to false so that the next data set encounters the next location tag first.

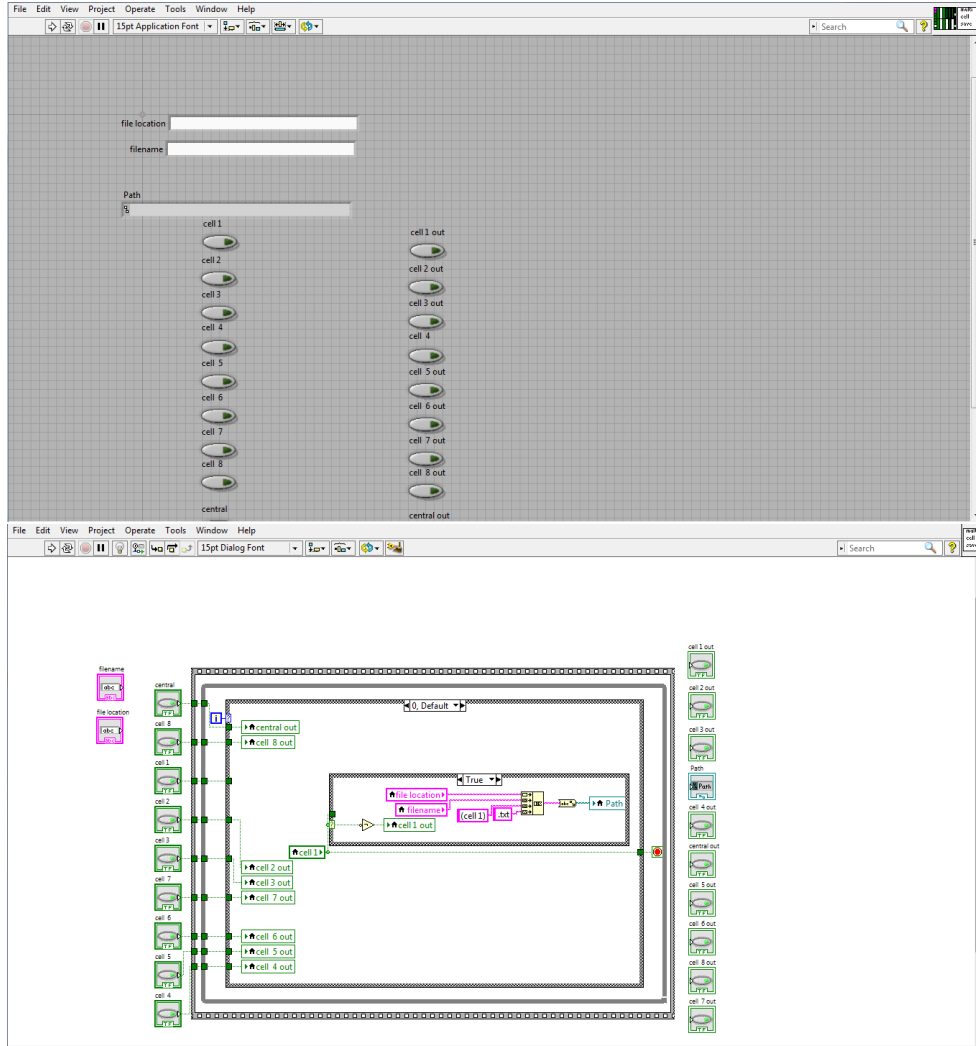


Figure 16: **Top** The front panel for *new SAVE.vi* showing the user specified input controls for the target locations to test and the output indicators showing the updated target sites based on which ones have already been completed. **Bottom** The block diagram which shows the internal structure of the VI. Each boolean input corresponds to a cell location and is tied to a particular identifying string to be added to the data file for that particular location

## 5.2 Sample Path Determination

The versatility of the SAMM device means that there are a number of different electrical pathways that must be coordinated to ensure proper functionality. There are three distinct points at which *Framework.vi* must determine which electrical pathway to connect: the different anodic connections on a single cell based on what specific locations are to be tested on each cell (only an issue for dry cells for which the SAMM supports up to eight different testing sites), the connections between each cell holder attachment based on what cell type is being tested, and the pathway between the DAQ 6221 for IPCE measurement and the Gamry REF-600 potentiostat for IV/EIS analysis.

The anodic electrodes on a dry cell are mechanically connected by eight separate contact pins which feed into the NC pins of 8 different relays on a terminal block controlled by the PCI 6520 relay. The subVI *PCI cell switches.vi* controls which anodic

pathway is currently connected based on the cell locations to test specified by the user. It uses the same logic structure as *new SAVE.vi* to determine which anode connection should be active and which have already been tested using the current measurement.

*Framework.vi* must also be able to form isolated connections between four different sets of anodes and cathodes depending on the type of cell being tested: sample SM1PD1B diode, liquid electrolyte cell, dry cell with contacts on same side, or a dry cell with contacts on opposite side. The subVI *sample path switch.vi* addresses this need. The sub VI takes four boolean inputs which correspond to the four types of cell that can be tested. Each of these boolean inputs is translated into a digital signal using the DAQ 6221 that triggers the switch to connect the appropriate pathway. Three ELK 924 switches and one pin set from a PCI 6520 relay were used to accomplish this.

Finally, the path selection corresponding to which device is being used for data acquisition, Gamry for IV/EIS measurement, DAQ 6221 for IPCE measurement, is controlled by another ELK 924 switch. Again, another digital I/O pin on the DAQ 6221 is used to trigger this switch.

### 5.3 Motor Control

The SAMM requires two distinct types of motion. The armature supporting the two light sources, the monochromatic light and the broad spectrum white light, rotates to allow the appropriate light for each test to be aimed directly at the sample. Also connected to a mobile stage, the sample is moved translationally in the plane perpendicular to the incident light. For cells with multiple active sites, this allows for isolated excitation of each anode. Two VI's handle this motion: *Intrasample movement.vi* directs the translational motion of the stage and *programmed arm rotation.vi* controls the rotation of the light source armature. *Intrasample movement.vi* communicates with two Thorlabs T-cube stepper motors which handle motion in the horizontal and vertical directions to each of the discrete locations to be tested. This VI is called between each measurement using information about which cells have already been tested output by *new SAVE.vi*

*Intrasample movement.vi* takes two controls as the XY coordinates the current target position. It then communicates this to the two stepper motor controllers which power individual actuators mounted on the stage.

*programmed arm rotation.vi* directs the rotation of the light source armature. There are three distinct positions for the armature to be in depending on which test is being performed. Its default position is for the monochromatic light to be centered on the sample while the MWWFH1 is positioned about  $12^\circ$  counterclockwise. This is the at which the SAMM performs IPCE measurements under dark conditions. For IV and EIS measurements, the arm is rotated  $12^\circ$  clockwise so that the white light of the MWWFH1 can be directed perpendicularly on the sample. For a sun biased IPCE measurement, the armature is rotated so that both the monochromatic light and the MWWFH1 are about  $6^\circ$  off center to either side. Another subVI, *IPCE solar-nonsolar ctrl.vi* takes the user specified testing sequence and ensures that the rotational arm rotates to the correct position regardless of which tests have already been performed. The complexity of *programmed arm rotation.vi* is due to the fact that four different types of frequencies of

signal are sent using four different outputs of the DAQ 6221 depending on the direction and magnitude of movement. These have all been preset using arrays of boolean values corresponding to each type of movement that is required.

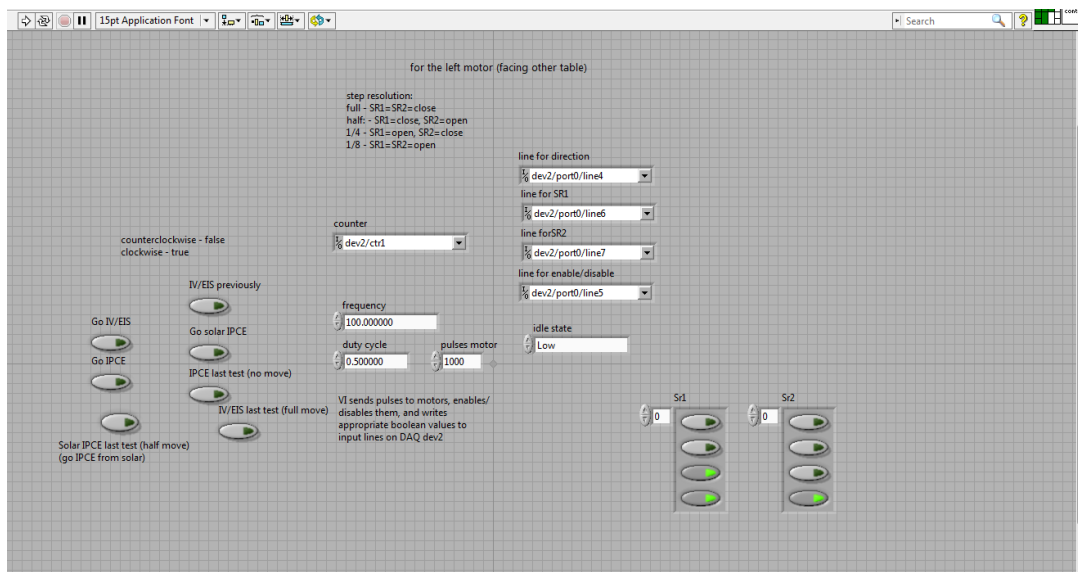


Figure 17: The front panel for *programmed arm rotation.vi*. The boolean controls correspond to the different motions required of the armature during use. When motion has terminated, these values should match up.

This subVI draws from a VI written specifically to control the custom built stepper motor controlling the light source armature rotation.<sup>17</sup> It interprets the boolean controls corresponding to each motion required for the arm rotation. It then communicates with the motor using several of the DAQ 6221's digital I/O pins.

## 5.4 I-V Curve Analysis

IV curve analysis requires communication to the Gamry REF-600 potentiostat via a USB connection. From the user interface in LabVIEW, the user is able to set all of the experimental parameters for the test which are then executed by the potentiostat. An example program provided by Gamry was heavily modified to integrate into *Framework.vi*.<sup>18</sup> To do this, the Gamry communication structures had to be extracted from the built-in experimental procedure and user interface commands. Additionally, a number of other tests were programmed into Gamry's program which required a variety of electrodes to the sample. These had to be removed as well since the SAMM does not currently have the infrastructure to support that number of pathways. Figure N shows the front panel of the Gamry sample program which is very different from the front panel of *Framework.vi*. Additional VI's to save the measured IV data to a standardized path were also written and integrated into *Framework.vi*. Most significant to IV curve analysis, the program allows the user to input the file name for the saved data as well as control the range of applied voltages to scan through, the rate of scanning in V/s and the data collection frequency. A number of other Gamry settings may also be controlled for more delicate tests.

## 5.5 EIS

The LabVIEW structure for EIS was incorporated much the same way as the IV structure. A sample program provided by Gamry<sup>19</sup> was modified to allow integration into the loop structure of *Framework.vi* and additional subVIs were written to handle data recording and The program allows the user to control the frequency range of the excitation signal, DC offset, amplitude, and target impedance range. The EIS experimental sequence is structured differently than the IV sequence. Generating an IV curve requires the application of only one DC signal in which the voltage level scans through the range set by the user. The IV curve data acquisition all occurs during one execution of its internal sequence. Because EIS must apply a number of different excitation signals across the frequency range set by the user, it executes its entire signal application and measurement operation for each data point and then resets. Because of the difference in structure, it was necessary to add an additional structure to the VI *new SAVE.vi* called *new SAVE for EIS only.vi*. This subVI reads a boolean indicator at the input which indicates whether the EIS measurement sequence has completed. If this indicator is FALSE, the cell location being tested is not removed from the array of cell locations to visit and next data point is also added to the same file. If this indicator is TRUE, then the current cell location is removed from the target site array and no more data is added to that file.

## 5.6 IPCE Measurement

The IPCE portion of *Framework.vi* handles IPCE calibration operations, as well as both dark and sun biased IPCE measurements. The two main operations within this part of the program are the monochromator communication structures and the data acquisition structures. The monochromator can only be connected to one computer at a time and is currently integrated into another system elsewhere in the laboratory. In order to get around this, a TCP-IP connection must first be made to the computer connected to the monochromator. Once the connection is made, the monochromator can be controlled using LabVIEW from the computer connected to the SAMM. Efforts to control the monochromator through LabVIEW had been made previously and so much of the communication and wavelength setting structure was integrated from another VI.<sup>20</sup> These structures allow for wavelength specification, filename determination, and specification of the number of discrete data points to take during the data acquisition process.

Data acquisition occurs in several steps. First, a calibration data set is created each day an IPCE measurement is taken. This is accomplished by inserting the SMW1PD1B diode into the SAMM and running the IPCE calibration and Solar IPCE calibration sequence found on the last page of the front panel. This creates a set of reference data points that prevent any changes in the electronic hardware, like battery drain, from skewing the measured data. This data set, along with a matching data set of the reference diode from the second light exposure path (figure 12) is used as a multiplier on the measured voltage from the sample being tested. This ensures that intensity variation between wavelengths doesn't skew the IPCE curve generated. The subVI, *IPCEvoltmeter 2.vi* handles the actual signal voltage signal measurement. First, the voltage signal at the output of the amplifying circuit described in section 4.5 is passed into an analog input pin of the DAQ 6221. This signal is first time averaged to eliminate any remaining effects of random noise.



A Fourier transform is then performed on the signal to disassemble it into its frequency components. The magnitude of the signal at 270 Hz, the frequency of the chopper within the monochromator, is the one that is actually recorded as the IPCE data point.

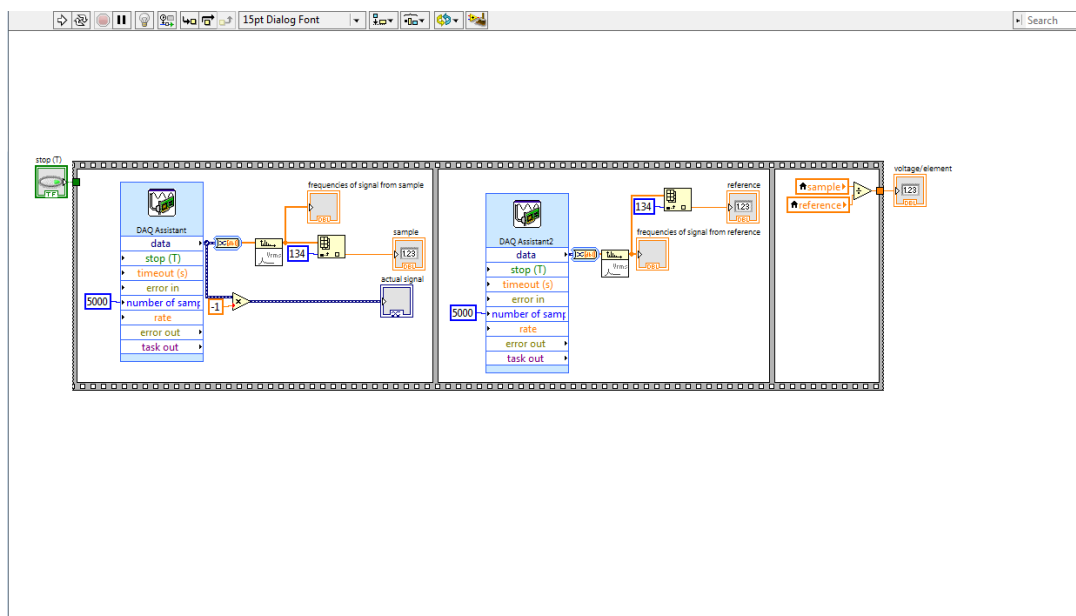


Figure 18: The block diagram of *IPCEvoltmeter 2.vi*. This subVI operates in 3 stages in which it acquires 10,000 samples of the signal being output by the sample as well as the reference diode and performs a Fourier transform to isolate the 270 Hz signal resulting from the monochromatic excitation.

## 6 Experimental Procedure

Detailed activation and troubleshooting procedures are provided in appendix III however the general operation of the SAMM is described in this section. After ensuring that everything is powered on and operating correctly, the user will first insert the SMW1PD1B sample diode and perform the IPCE calibration tests. These must be performed once each day an IPCE measurement is taken to generate reference data curves that are used to correct for changes in the hardware electronics and monochromatic light intensity variations. Afterwards, the user may detach the sample diode and insert the cell holder that is appropriate for the cell they are testing. The cell holder features a clip on the side that may be closed on the front of the holder to form an anode connection on the front of the cell. As discussed in section 2.2, this is so that opaque cells can be characterized in addition to transparent cells. After the sample has been loaded into the SAMM, the user may run *Framework.vi*. At this point, the program will initialize all of the hardware but it won't execute any measurement sequences until the green START button on the first page of the front panel is toggled. The user can select which tests they wish to perform by toggling the boolean control at the top of each page. The other controls on each page may be used to specify any other test parameters desired. The user must also specify a filename for the saved data sets for each test. Once everything has been set, the user will click START and the SAMM will perform the rest of the experimental sequence automatically. Depending on what sequence the user has fed into the program, the length of the experimental sequence can vary greatly. IV curve measurement is very quick and

takes no longer than 15-20 seconds. A single EIS data run usually takes 1-2 minutes but can take longer if an unusually wide range of excitation signal frequency is specified. The IPCE sequence takes the longest to execute as time must be allowed for the monochromator to switch between the various wavelengths and needs about 3 minutes to execute completely. This means that the maximum length an experimental sequence can take, in which each test is repeated eight times, would take about 40 minutes. Gathering the same amount of data using the current infrastructure would take several times longer.

## 7 Conclusion and Next Steps

It is hoped that the SAMM will increase the efficiency of solar cell research here at the UNC EFRC. One project that has been planned with the SAMM in mind is to investigate the effect that dopant concentrations have on photoanode films. Properly measuring this requires testing a single cell at multiple locations which is something only the SAMM can conveniently do. Furthermore, currently titanium oxide ( $\text{TiO}_2$ ) is the most thoroughly investigated metal oxide but other oxides like strontium titanate ( $\text{SrTiO}_3$ ) and niobium oxide may also be tested.

There are also a few areas in which the operation of the SAMM can be improved. Manual control of the translational motors should be added in the experimental setup of the program rather than requiring each location to be tied to a boolean control. However, because the motors have been non-functional, this update has been postponed. The present design of the wet cell holder supports only one connection at a time. The addition of several more loose clips which can be attached at any site desired and given manual locations during experimental setup would allow for maximum flexibility of the wet cell capabilities. Currently the dry cell holder can only accommodate one anodic connection per opaque sample and the addition of more would allow the SAMM to characterize opaque cells with the same efficiency as transparent cells. Additionally, the cell holders can only conveniently hold cells that are about 1"x1". Smaller cells tend to slip between electrode connections or may not even reach the clamping surfaces that hold larger cells in place. Allowing for a larger variety of cell sizes would also improve the flexibility of the SAMM. The addition of another detector on the opposite side of the sample cell holder would also allow for measurement of the amount of transmitted light, light that passes through the cell without being absorbed, to characterize the transparency of the cell.

Finally, it would be a great improvement to increase the flexibility of the IPCE measurement by allowing for customized ranges of wavelengths to be tested. Currently the only wavelength range that can be tested is 350 nm to 1150 nm with a resolution of 10 nm since that is the set of reference data that is used by the program as a multiplier for measured data. However, if a best fit curve could be generated to allow for values to be calculated for values between each data point, then researchers could test their cells at a much higher resolution of wavelength behavior. Figure 19 shows a first pass at achieving this using a polynomial best fit. However, clearly the fit is not perfect and so the method of cubic splines will be explored in order to increase the accuracy of the best fit.

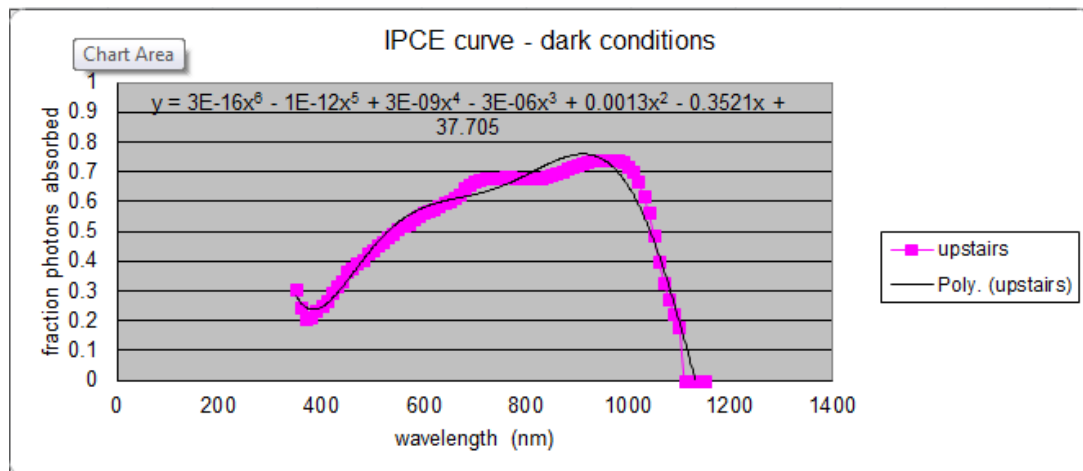


Figure 19: a polynomial best fit curve generated in excel. The accuracy is not ideal so a cubic splines method will be explored to improve the accuracy of the curve

## 8 References

This project was partially funded by the UNC Honors College through the Dunlevie Honors Undergraduate Research Fund

- [1] Grimes, Craig A., and Oomman K. Varghese. "Hydrogen from Water Using Renewable Energy." *Light, Water, Hydrogen the Solar Generation of Hydrogen by Water Photoelectrolysis*. New York: Springer, 2008. Print
- [2] "Creating Tomorrow's Solar Fuels Today." UNC EFRC – Center for Solar Fuels. University of North Carolina at Chapel Hill, 1 Jan. 2013. Web. 15 Mar. 2015. <<http://www.efrc.unc.edu/>>
- [3] Chen, Y.L., Y.J. Ma, D.D. Chen, W.Q. Wang, and K. Ding. "Effect of Graphene on Photoluminescence Properties of Graphene/GeSi Quantum Dot Hybrid Structures." *AIP* 105.2 (2014). AIP Scitation. Applied Physical Letters. Web. 13 Mar. 2015. <<http://scitation.aip.org/content/aip/journal/apl/105/2/10.1063/1.4889890c>>.
- [4] Muller, Richard S., and Theodore I. Kamins. "Semiconductor Electronics." *Device Electronics for Integrated Circuits*. 2nd ed. New York: Wiley, 1986. Print.
- [5] Hagfeldt, Anders, Gerrit Boschloo, Licheng Sun, Lars Kloo, and Henrik Pettersson. "Dye-Sensitized Solar Cells." *Chemistry Review* 110 (2010): 6595–6663. Applied Materials and Interfaces. ACS Publications. Web. 7 Mar. 2015. <<http://pubs.acs.org/doi/pdfplus/10.1021/cr900356p>>
- [6] Gao, Xiang-Dong, Xiao-Min Li, and Xiao-Yan Gan. "Enhancing the Light Harvesting Capacity of the Photoanode Films in Dye-Sensitized Solar Cells." *Solar Cells - Research and Application Perspectives*. INTECH Open Access, 2013. Print.
- [7] Ghosh, Rudresh, M. Kyle Brennaman, Edward Samulski, Thomas Meyer, and Rene Lopez. "Nanoforest Nb2O5 Photoanodes for Dye-Sensitized Solar Cells by Pulsed Laser Deposition." *Applied Materials and Interfaces* 3 (2011): 3929–3935. ACS. ACS Publications. Web. 12 Mar. 2015. <<http://vb3lk7eb4t.search.serialssolutions.com/>>
- [8] "Interpreting IV Curves." Application Note PVA-600-1: Guide To Interpreting I-V Curve Measurements of PV Arrays. Solmetric, 2011. Print.
- [9] Ulgut, Burak. "Basics of Electrochemical Impedance Spectroscopy." Gamry Instruments, 12 Feb. 2014. Web. 21 Mar. 2015. <<http://www.gamry.com/index.php/application-notes/basics-of-electrochemical-impedance-spectroscopy/>>.

- [10] Brogan, Shane. "Wet Cell Holder Fabrication." 2014 - 2015.
- [11] "Fiber-Coupled LED Features." Fiber-Coupled High-Power LEDs. Thor-Labs, 1 Jan. 2015. Web. 26 Mar. 2015. <<https://www.thorlabs.com>>
- [12] Honsberg, Christiana, and Stuart Bowden. "Standard Solar Spectra." PV Education. 1 Jan. 2013. Web. 15 Mar. 2015. <<http://www.pveducation.org/pvcdrom/appendices/standard-solar-spectra>>
- [13] "Signals, Filters, and Amplifiers." Principles of Electronics, Analog and Digital. Orlando: Harcourt Brace Jovanovich, 1987. Print.
- [14] "Multiple Feedback Band-pass Filter Design Tool." OKAWA Electric Design. OKAWA, 1 Jan. 2008. Web. 17 Mar. 2015. <<http://sim.okawadenshi.jp/en/OPtazyuBakeisan.htm>>
- [15] "User Guide NI 6520/6521." (2007). National Instruments. Web. 1 Mar. 2015. <<http://www.ni.com/pdf/manuals/372280a.pdf>>.
- [16] "ELK-924 Sensitive Relay." ELK. ELK Products, 1 Jan. 2015. Web. 20 Mar. 2015. <<http://www.elkproducts.com/product-catalog/elk-924-sensitive-relay>>.
- [17] Tumbleston, John. "general pulses motor.vi" 2010.
- [18] VFP600.vi. National Instruments LabVIEW Virtual Instrument program. [Http://www.gamry.com/](http://www.gamry.com/). 1 Jan. 2012. Web
- [19] LVEIS.vi. National Instruments LabVIEW Virtual Instrument program. [Http://www.gamry.com/](http://www.gamry.com/). 1 Jan. 2012. Web
- [20] Tumbleston, John. "The program - angular measurement.vi" 2010.

## 9 Appendix

### 9.1 I. User Interface

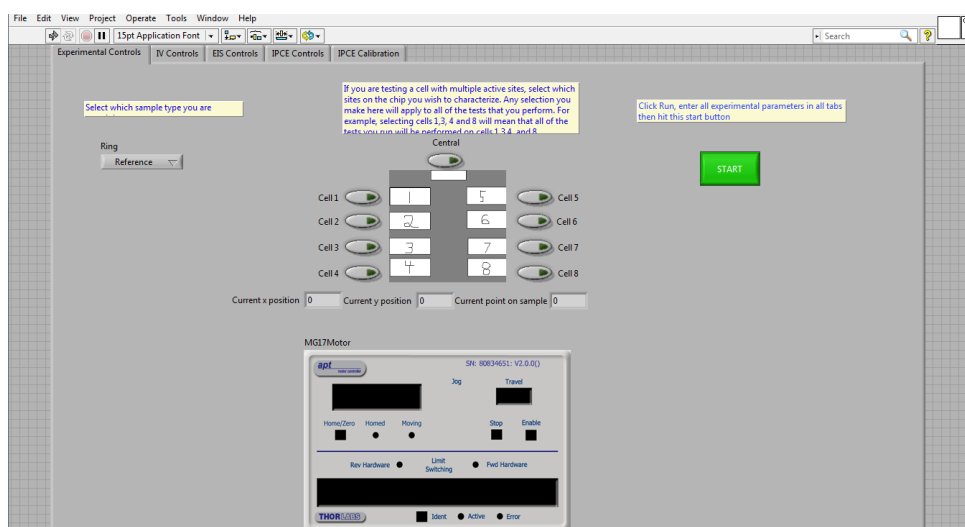


Figure 20: The main page of the SAMM Framework program. On the left is the control for the type of cell and cell holder being used, in the center is the location on the cell to be tested, and on the right is the START command that launches the testing once all experimental parameters have been set. The indicator at the bottom merely indicates connection to the Thorlabs T-cube stepper motors

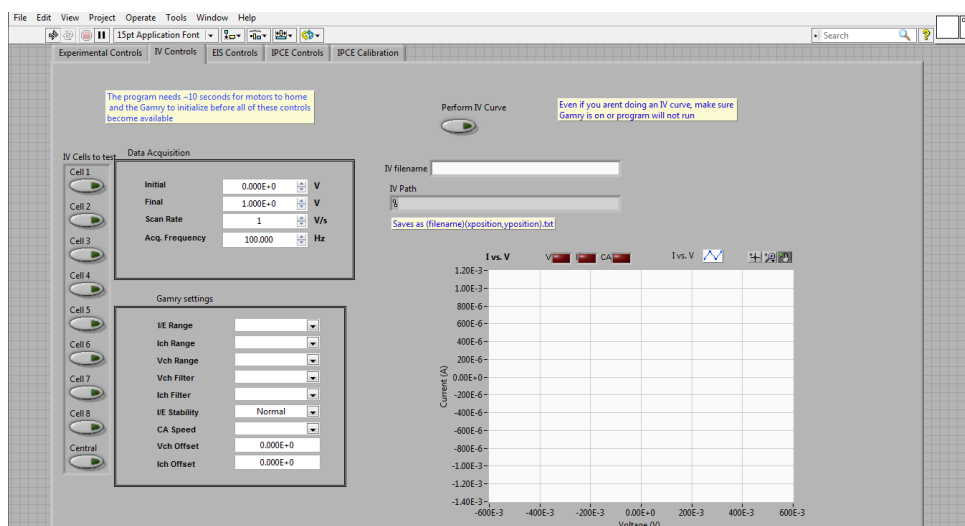


Figure 21: The controls for IV measurement. The array of boolean indicators on the left displays the cell locations to be tested. Adjacent to them are the user specified parameters like voltage scanning range and data acquisition frequency. To the right is the string control where users input the desired file name for the saved data while the graph directly below this is where the data is actually displayed



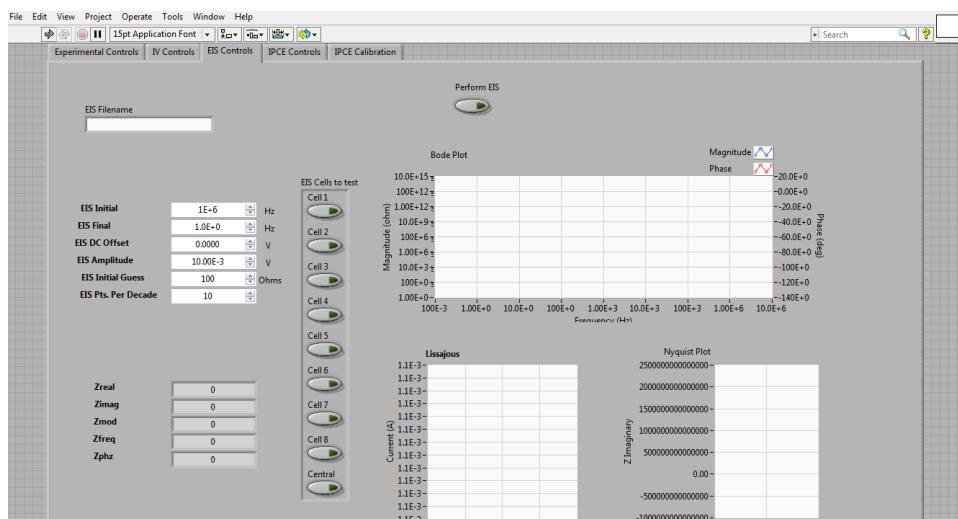


Figure 22: The controls for the EIS measurement path. As before the array of boolean indicators display the cell locations to be tested. On the left are the user specified inputs like data file name and frequency range of the applied the excitation signal. On the left are the charts for the Lissajous (lower left), Nyquist (lower right), and Bode plots (top middle)

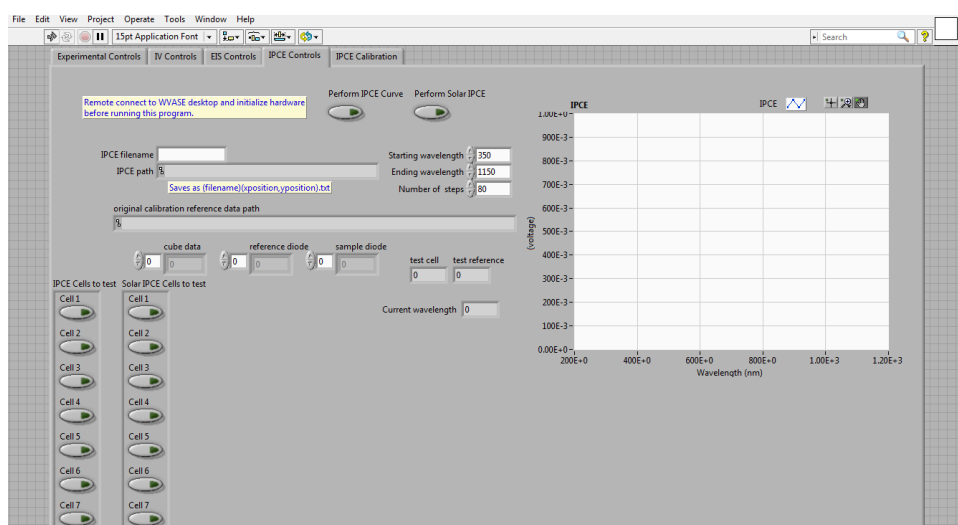


Figure 23: The controls for IPCE measurement. As before, on the left are user inputs like data filename, wavelength range to scan the monochromatic light through as well as indicators for the current wavelength, saved filepath, and data point number. On the right is the chart to display the IPCE data. At the top center are two boolean controls to specify the lighting regime to use. If both Non-Solar and Solar are selected, the SAMM will perform a sun biased IPCE measurement followed immediately by an unbiased measurement

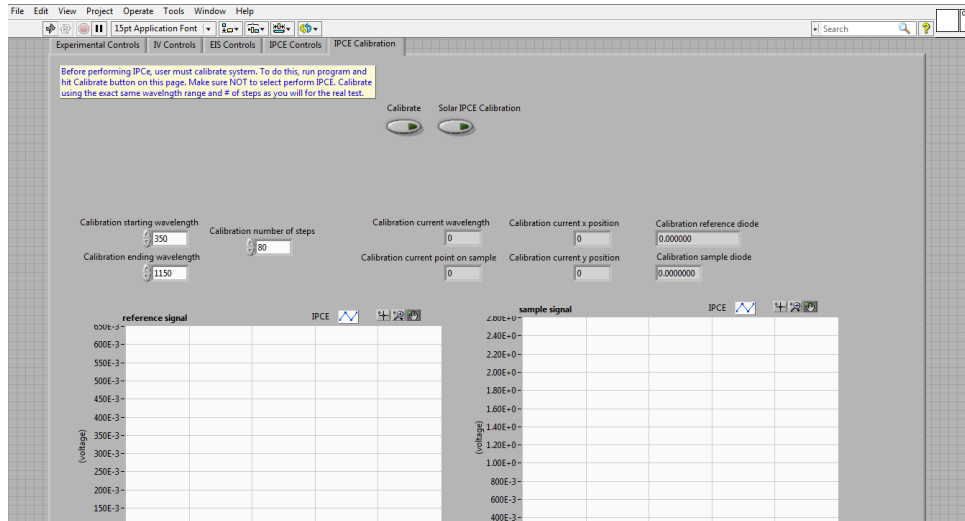


Figure 24: controls for IPCE calibration operation. This must be performed before any IPCE measurement can be taken to account for small changes in the circuit conditions of the cell response signal (ex. battery depletion) The controls are very similar to the controls for the actual IPCE measurement operation. The additional chart displays the signal form the reference diode that forms the second optical pathway to capture intensity variations between wavelengths in the monochromatic light

## 9.2 II. Equipment Used

### Sampling

- Dry cell holder attachment
- Liquid electrolyte cell holder attachment
- Thorlabs SM1PD1B diode for calibration

### Motion

- Custom stepper motor for arm rotation
- 2 Thorlabs T-cube Stepper motors with linear actuators

### Signaling

- 2 PCI 6520 Relays
- 4 ELK 924 Switches
- National Instruments 6221 Data Acquisition Device

### IV curve analysis

- Gamry REF-600 potentiostat (also used for EIS)
- Thorlabs LEDD1B diode driver with MWWFH1 Warm White light diode and controller (also used for sun biased IPCE measurement)

### IPCE Measurement

- Thorlabs SM1PD1B diode for corrective baseline intensity data
- Woollam VASE Monochromator
- Portable Technologies PTA-100 Transimpedance Amplifier
- MINMAX ABF-04D12 Dual Output Power Supply
- Custom amplifying filter circuit for sun biased measurement

## 9.3 III. Startup Procedure

### Turn On

- WVASE Ellipsometer control module
- GAMRY REF-600 potentiostat
- Monochromator Power - wait a few seconds to warm up then turn on lamp and ignition
- Project box – flip switch and set Transimpedance Amplifier to  $10^{-6}$
- Rotational Arm custom stepper motor control box

### Plug In/Hardware

- Two motors – open APT User to verify functionality. Click home to reset to their default position
- Ensure that the orange fiber optic cable running from lights source arm to the Monochromator is connected
- Connect the W/WS (green/blue) leads of the gamry to the green wire labeled ‘anode’ and the C/R (red/white) leads to the white wire labeled ‘cathode’
- Make sure the light source tower arm is centered using the mark at the base. This ensures that all subsequent automated rotational motor commands will be calibrated to the correct position

### Software

#### Monochromator

- Remote connect to other desktop from start menu
- IP - 192.168.0.8
- Username – ellipsometer
- Password - 9199626828
- Start WVASE program on desktop
- Initialize hardware
- Move monochromator to white light to verify

#### Gamry

- Open Gamry Framework and verify communication to REF-600

### Framework

#### IPCE

- Run calibration first before testing/ DAILY
- set wavelength regime to 350-1150

- IV
- Select voltage range, sample speed and acquisition rate
  - Set I/E range to highest (600 mA)
  - Set CA speed to normal

### EIS

- Uses same connections at IV tests

### Generally

- Run program, allow 5 seconds for parameters to initialize

- Toggle each test you wish to perform and specify parameters then hit start on main tab
- Select location to be tested on each cell and what type of cell you are testing
  - Dry vs wet, electrodes on same side vs opposite sides
- Do not manipulate LabVIEW while translational motors are running – motor control freezes and Framework program may crash

## 9.4 IV. SubVI's

### Sample Path Selection

- **sample path switch.vi** - Controls one PCI 6520 relay and 3 ELK 924 switches to determine which sample pathway is connected based on the user's selection of cell type and holder attachment.
- **PCI cell switches.vi** - Controls one PCI 6520 relay to determine which location pathway is connected of the multiple pathways of dry cells that have more than one active area. Dependent on user's selection of measurement locations.
- **IPCE\_IV switch.vi** - Controls an ELK 924 switch to alternate between the connections to the IPCE measurement pathway and the IV/EIS pathway.

### Motion

- **IPCE solar-nonsolar ctrl.vi** - controls the motion of the light source arm to position the light sources correctly for IPCE measurement while taking into account whether or not an EIS or IV test had been done previously
- **programed arm rotation.vi** - controls a custom stepper motor to rotate the light sources as dictated by the measurement being performed.
- **intrasample movement.vi** - Controls the two Thorlab T-cube stepper motors to
- **movehome.vi** - A cleanup VI that directs the Thorlabs T-cube stepper motors back to their default positions at the end of a testing cycle.
- **locked motor control and movement.vi** - used to calibrate the discrete locations on a single cell that should be tested

### Data recording

- **New SAVE.vi** - Generates an array of strings that can be attached to each tests saved data file as a string that identifies it according to its location on the tested cell
- **IV Save.vi** - saves the IV data according to the title string specified by the user and any additional identifying tags added by the SAMM program (ex. active site location)
- **New SAVE\_EIS only.vi** - modified structure of New Save.vi to take into account the looped nature of the EIS portion of the SAMM program

### IV curve analysis

- **white diode activation.vi** - Activates a Thorlabs LEDD1B white diode. This is also called during sun biased EIS and IPCE measurement

### IPCE Measurement

- **IPCE voltmeter2.vi** - controls the data acquisition during IPCE measurements so that each wavelengths data point is an average of 1000 samples of the signal at 273 Hz, the particular frequency of the oscillating monochromatic light, which is isolated using a Fourier transform